Memoirs of the School of Engineering, Okayama University Vol. 17, No.1, February 1983

Off-Line Stereo Plotting by Means of Image Correlation

Chuji MORI*, Susumu HATTORI* and Shinya HAMATE**

(Received November 9, 1982)

Synopsis

The algorithm of automatic stereo plotting by iterative image correlation from aerial photographs and the corresponding empirical tests are described. The algorithm is oriented to off-line process, using a image scanner and a general purpose computer, and consists of 3 hierarchical correlation steps, based on one-dimensional matching using usual correlation maximum. For the correlation calculation, the FFT is effectively used. Though some defects exist in the algorithm at present, close contour plotting to middle scale maps is available except in hilly regions, in which marked features in ground covers do not exist.

1. Introduction

Some methods of automatic stereo matching of aerial photographs (identifying the conjugate image points in a stereo pair) have been investigated for the purpose of automation in photogrammetry. It can be said from these investigations, that relatively precise matching might be possible with image correlation techniques in the case of middle or small scale photographs. In the case of automatic stereo plotting, various, systematic and speedy matchings are necessary for reconstructing three dimensional models of terrain. Up to now, some special purpose devices for the production of ortho-photos and digital

* Department of Civil Engineering
** Yakumo Constructional Consultants Co. Ltd.

terrain models (DTM), based on image correlation, have already been developed semi-commercially (e.g.,by Gestalt Co.[1], Bendix Co.[2] and Zeiss Jena Co.[3]). These devices are far from ideal for practical requirement and need further developments and improvements.

The same kind of processes are feasible in off-line process using a scanning micro-densitometer and a general purpose computer, which are at present available in any laboratory. In some cases, however, general purpose computers do not have the capability to perform differential rectification of photographs to produce ortho-photos or DTMs practically. But in principle, there are no differences between on-line and off-line process. Therefore, off-line correlation is significant as a base for development of special-purpose devices.

Since off-line stereo plotting was originally introduced by Sharp (IBM) in 1964[4], some investigators have offered subsequent reports dealing with off-line stereo plotting[5],[6],[7], Keating, et al.[8], published the improved method of processing from two-dimensional correlation for orientation, to one-dimensional correlation for final matching. Panton, et al.[9], showed the new design of an array processor for high speed correlation and the sophisticatied correlation algorithm designed to eradicate perspective distortions.

The off-line methods offered up until now, however,are based on point by point matching. On the contrary, this algorithm is based on iterative image correlation, patch by patch. This paper describes the algorithmic approach as well as some results of correlation tests.

The largest hindrances in the correlation of aerial photographic images are the image noise due to variations of directional reflectance of ground objects or vignetting in the optical system and the perspective distortions due to the reliefs of the terrain (including buildings, cliffs, etc.). This paper places stress on the latter problem. The algorithm developed is designed to eliminate the perspective distortion on the image by iterative correlations using the Fast Fourier Transform (FFT) and at the same time to decide the x_c-parallax distribution on the image to reconstruct the terrain reliefs.

2. The Flow of off-line Stereo Plotting

The off-line stereo plotting system consists of photo digitizing, image correlation and contour plotting. In this system, as distinguished from on-line system, it is very useful for image correlation to rectify the stereo images though preprocessing. For this reason

the processing flow in the system may be expressed as shown in Fig.1.

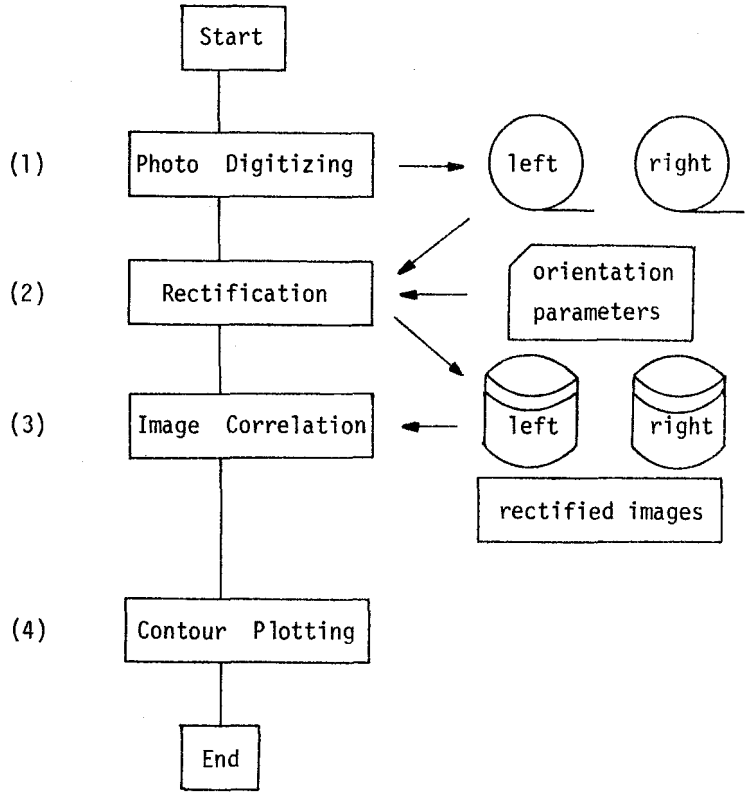

Fig.1 Flow Chart for Stereo Plotting

(1) Photo digitizing

It is most desirable that a photograph is scanned in such a way that the (digitized) image coordinate system *row column* coincides with the photographic coordinate system $x\ y$. Otherwise, the relation between the two coordinate systems should be specified by use of the coordinates of fiducial marks in the margin of the photograph. For simplicity in the subsequent discussion, both systems are assumed to coincide and the photographic coordinate system is used alternatively.

(2) Rectification[10]

In aerial photography, camera axes are inevitably deviated slighly from vertical, and during flight course exposure heights are not the same. The mutual positional relations of the photographic coordinate systems $x_1\ y_1$ and $x_2\ y_2$ (the left and right images respectively), the model coordinate system $X\ Y\ Z$ and the ground coordinate

system X_G Y_G Z_G are schematically shown in Fig.2.

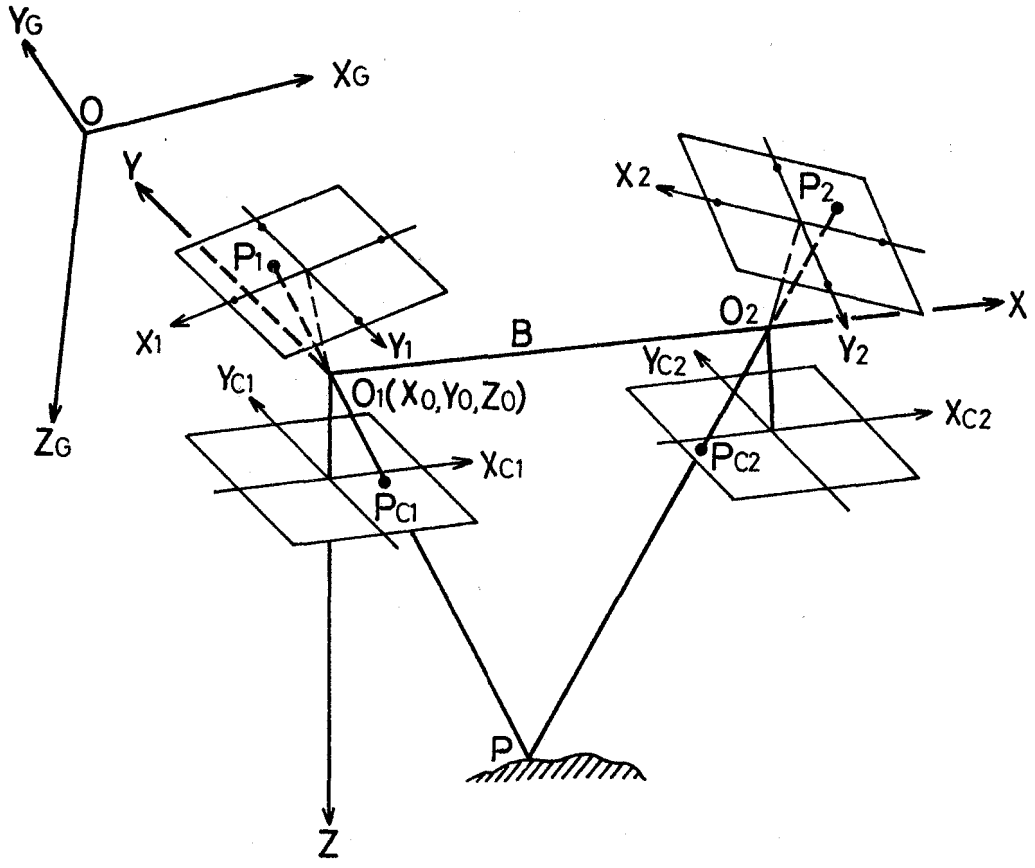

Fig.2 Coordinate Systems and Rectifications

The photographic coordinate axes are so defined that they pass through the fiducial marks and the principal points of the respective photographs. The model coordinate system is defined such that the origin O_1 coincides with the projection center of the left photograph, and the X-axis coincides with the air base, $\overline{O_1 O_2}$.

The rectification intends to reproject the stereo image pair to a plane parallel to the XY-plane. Let x_{c1} y_{c1} and x_{c2} y_{c2} be the rectified image coordinate system, and the x_{c1}-axis and x_{c2}-axis be in a straight line parallel to the X-axis. Thus it becomes guickly apparent, a pair of conjugate points on the rectified images have the

same y_c coordinates. This property is very useful to correlate the image data stored in sequential files. This idea was first presented by Kreiling[11].

The rectification process requires the principal distance c and the rotation matrces D_L and D_R of the left and right images associated with the X,Y,Z-axes respectively. The rotation matrices D_L and D_R, as well as the rotation matrix D and the translation X_0, Y_0, Z_0 of the model coordinate system associated with the ground coordinate system, can be simultaneously obtained from the results of aero-triangulation.

The relations of (x_{c1}, y_{c1}) with (x_1, y_1), and of (x_{c2}, y_{c2}) with (x_1, y_1) are expressed by the projective equations.

$$\left.\begin{aligned} \begin{bmatrix} x_1 \\ y_1 \end{bmatrix} &= \frac{d_{L11}\, x_{c1} + d_{L21}\, y_{c1} + d_{L31}\, c}{d_{L13}\, x_{c1} + d_{L23}\, y_{c1} + d_{L33}\, c}\, c \\ \begin{bmatrix} x_2 \\ y_2 \end{bmatrix} &= \frac{d_{R11}\, x_{c2} + d_{R21}\, y_{c2} + d_{R31}\, c}{d_{R13}\, x_{c2} + d_{R23}\, y_{c2} + d_{R33}\, c}\, c, \end{aligned}\right\} \quad (1)$$

where d_{Lij}, d_{Rij} $(i=1,2,3; j=1,2,3)$ are the elements of D_L and D_R.

(3) Image Correlation

For reconstruction of the terrain reliefs, the coordinates of many reference points must be available, which might be placed either on the model datum, on the ground datum, or on the image plane. It this study, the reference points are located on a grid on the left rectified image, and their conjugates are subsequently searched for on the right image, according to the algorithm which consists of the hierarchical steps of the iterative correlations. The details will be explained in the subsequent section.

(4) Contour Plotting

If once the x_c-parallaxes of the reference points are given on the rectified images, there is no difficulty in plotting contour lines. Refering to Fig.2, the conjugate points $p_1(x_{c1}, y_c)$, $p_2(x_{c2}, y_c)$ on the rectified images and the ground point $P(X_G, Y_G, Z_G)$ can be related by the expressions:

$$\begin{bmatrix} X_G \\ Y_G \\ Z_G \end{bmatrix} = \frac{B}{P_{cx}} D \begin{bmatrix} x_{c1} \\ y_{c1} \\ c \end{bmatrix} + \begin{bmatrix} X_0 \\ Y_0 \\ Z_0 \end{bmatrix} \tag{2}$$

and

$$p_{cx} = x_{c1} - x_{c2}, \tag{3}$$

in which

p_{cx} : x_c-parallax between p_1 and p_2

B : air base on the ground

3. Algorithm for Image Correlation

Several algorithmic approaches for searching for pairs of conjugate points on the stereo images have been published. Almost all published algorithms are based on area matching. That is to say, the correlation window on the left image is matched to the search window on the right image. The algorithm in this paper, however, adopts the line matching method. Indeed, since S/N ratios in line matching are lower that in area matching, line matching is apt to lead to mismatch, but on the other hand it has an advantage of reducing computing time and of high sensitivity of indicating correlation peaks.

3-1 Correlation Procedure

On account of vignetting in the optical system or inhomogeneity of directional reflectance of ground objects, densitometric distortions intrude into the images. Such distortions can often be approximated locally by linear transfomation, employing a scale factor and a translation. Under linear transformation, a correlation coefficient is invariant. Hence, as matching correlation coefficients or correlation functions are exclusively used[12]. This algorithm also uses correlation functions.

As mentioned above, pairs of conjugate points can be searched for one-dimensionally, because they have the same y_c-coordinates. Thus the nodal points are located with equal spacing on the left image as shown in Fig.3, denoted by small circles. These points serve as reference points for reconstruction of the terrain.

In the case where the terrain is not flat, the x_c-parallaxes are

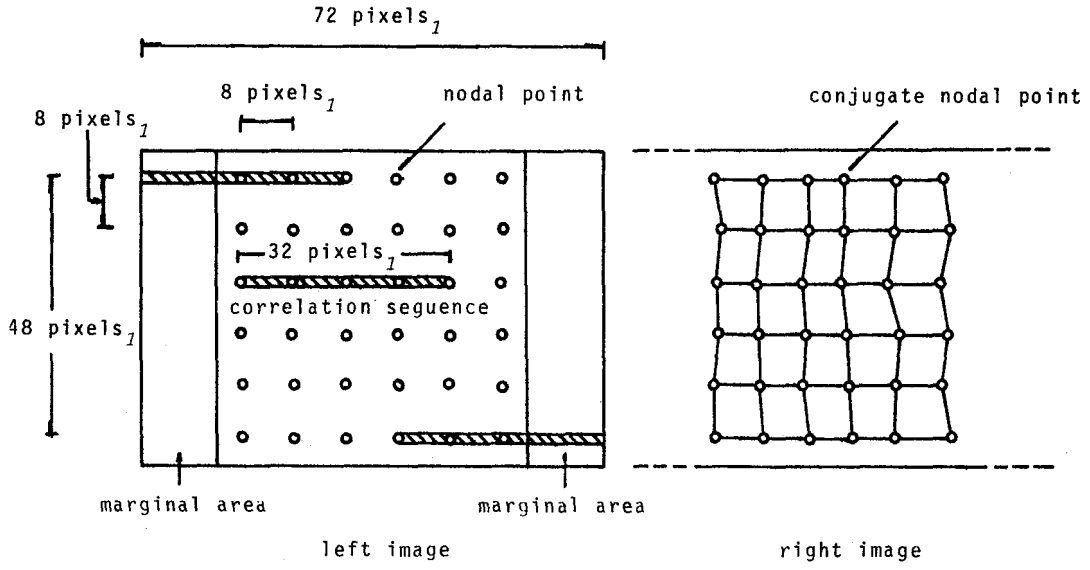

Fig.3 Nodal Points Allocation (the 1st Step)

not distributed constantly. And the location of the conjugate points on the right image fluctuate in the x_c-direction (see Fig.3). These projective distortions disturb correlations greatly. In order to resolve this problem, our algorithm is designed such that the right image is resampled to reconstruct the conformal image to the left (i. e., to indicate the homogeneous x_c-parallaxes to the left)by reffering to the estimated x_c-parallaxes in the last correlation, and the left image is correlated with the resampled image again to obtain more precise estimations of x_c-parallaxes. Although positive correlations cannot be obtained through initial sampling, by iterating this cyclic process, resampled images and estimated parallaxes are expected to converge gradually.

However, since no information about the terrain reliefs is given a priori, it is difficult to locate suitable search ranges of conjugates on the right image initially. Thus, the correlation process is constituted of three hierarchical steps, i.e., rough matching is performed at first on the coarse images with large pixels, and step by step it goes into detail on the fine images with small pixels.

To make explanations clear, suffixes are used for specifying the images or pixels of each step. Let the image$_i$ and pixel$_i$ denote the

image and of the i-th step ($i=1,2,3$).

Let pixel width of the original rectified images be d, and $pixel_1$ width is equal to $4d$, and $pixel_2$, $pixel_3$ width are $2d$ and d respectively. For each i-th step the nodal points are located on the left image with 8 $pixel_i$ spacing (see Fig.3). The estimated x_c-parallaxes in the i-th step are used as the initial values of the x_c-parallaxes in the $(i+1)$-th step. The allocation of the nodal points through 3 step is illustrated in Fig.4.

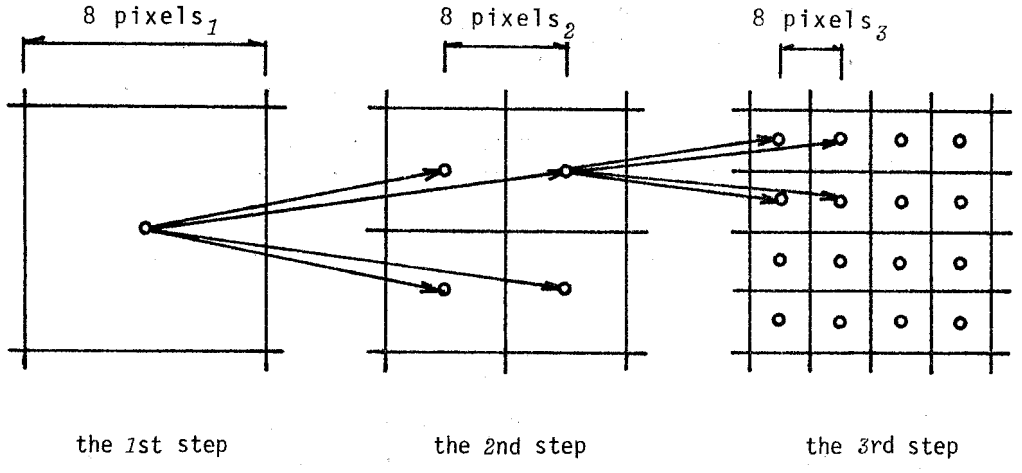

Fig.4 Initial Values Setting of the x_c-parallaxes
The estimated x_c-parallaxes in the i-th step are used as initial values of the 4 corresponding x_c-parallaxes of the $(i+1)$-th step.

Each square area is composed of 8 x 8 $pixels_i$, containing a nodal point at the center, is devided into 4 areas in the $(i+1)$-th step. Since it is impossible to correlate the entire plotting area at one time by reason of core memory limits of the computer, the left image is devided into overlapped rectangular sub-areas (termed correlation patches) and the plotting area is processed patch by patch.
One correlation patch, composed of 48 x 72 $pixels_1$ (the first step), 96 x 120 $pixels_2$ (the second step), and 192 x 216 $pixels_3$ (the third step) respectively, consists of a square area containing the nodal points and 2 marginal areas necessary for matching the nodal points in the border (see Fig.3). One correlation patch contains 6 x 6 nodal points in the first step, and 12 x 12 points, 24 x 24 points in the second and third steps respectively. The precision of estimated

x_c-parallaxes in the corner of patches may be considered less reliable. Hence, the patches are truncated such that 4 nodal points from each side (left,right, upper and lower) of the patch overlap each other. Fig.5 shows the overlapped allocation of correlation patches. At the end of the process 2 nodal points from each side are discarded. therefore, for plotting contour lines, only 400 points are available in each patch.

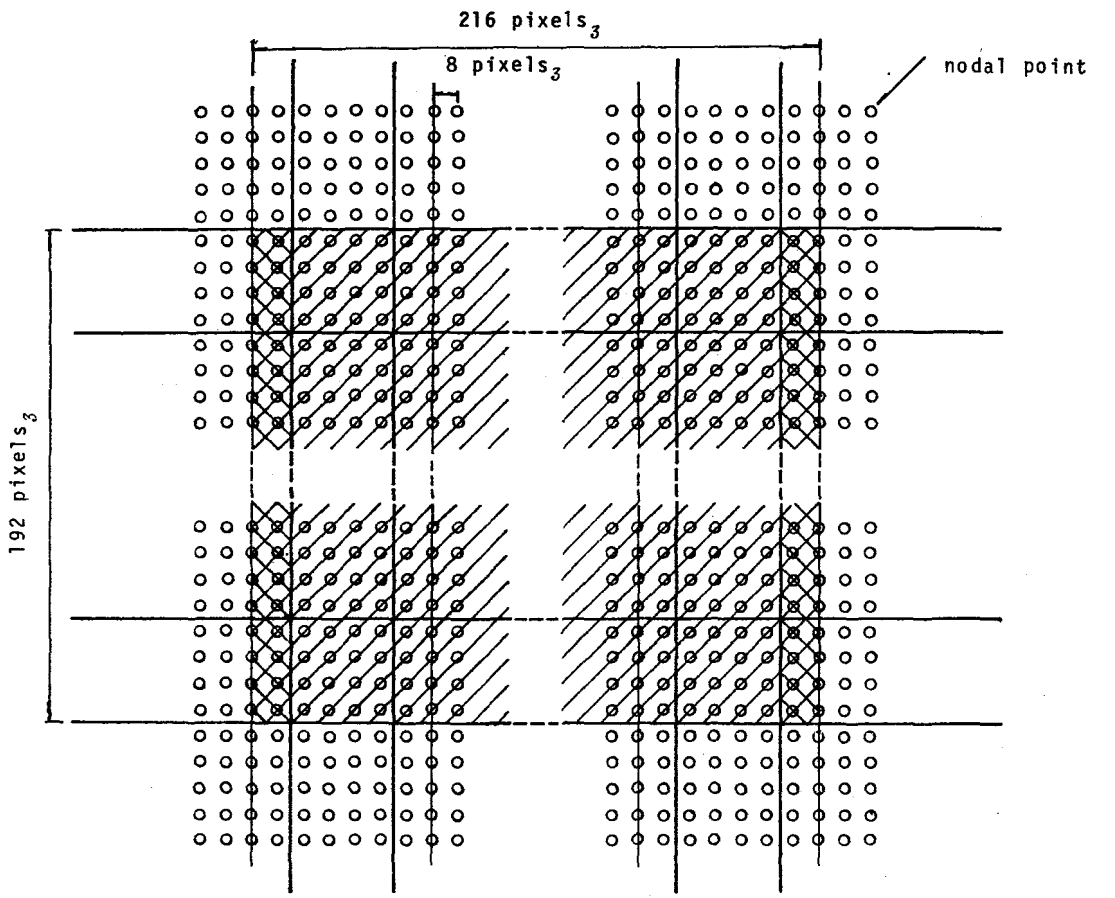

Fig.5 Overlapped Allocation of correlation patches (the 3rd step)
The hatched area denotes one correlation patch.
The maginal areas are double hatched.

On the other hand, the right image is divided into corresponding, overlapped search patches, the widths of which are changed in the x_c-direction, in order to fit the corresponding correlation patches, since the conjugate position of each correlation patch is not known precisely beforehand.

3-2 X_c-parallax Estimation

As the steps are the same in all cases, the estimation process of x_c-parallaxes is explained in conformity with the first step. The sequences of 32 density values, centered at p on the left image (see Fig.3), and another sequence of the same length on the right image centered at the predicted position of the conjugate of p, are picked up. They are then correlated to estimate the positional lags for correction of x_c-parallaxes. Let the left and right sequences be denoted by

$$u(n),\ v(n):\ n=0,1,\ldots\ldots,N-1\ (N=32)$$

respectively. The cross-correlation of $u(n)$ and $v(n)$ is defined as;

$$\left.\begin{aligned} R(\tau) &= \frac{1}{N}\sum_{n=0}^{N-1}(\,u(n)-u\,)(\,v(n+\tau)-v\,) \\ &= \frac{1}{N}\sum_{n=0}^{N-1}\bar{u}(n)\bar{v}(n+\tau), \end{aligned}\right\} \qquad (4)$$

where

$$u=\frac{1}{N}\sum_{n=0}^{N-1}u(n),\quad v=\frac{1}{N}\sum_{n=0}^{N-1}v(n)$$

$$\left.\begin{aligned} \bar{u}(n) &= u(n)-u \\ \bar{v}(n) &= v(n)-v \end{aligned}\right\}\quad n=0,1,\ldots\ldots\ldots,N-1.$$

and, $v(n)$ and $\bar{v}(n)$ are extended periodically with a period 32 beyond the defined domain. The size of the sequence designated above is determined so that the three quarters of the sequences overlap each other.

In our system, the 2-radix FFT is applied conveniently for calculation of cross-correlations[13]. However, since a large bias between the density levels of a pair of images exists in general, as compared with the signal variation, it should be resolved before correlation by subtracting the mean value from each element in the sequence in order to prevent false correlations.

On the rectified images, some residual y_c-parallaxes commonly remain. Therefore, for both images in the third step, averages of 3 density values in the y_c-direction are used as the elements of the sequences to reduce a defect due to y_c-parallaxes.

In the initial condition, the terrain is assumed flat, i.e., all x_c-parallaxes are set equal to the air base measured on the photograph.

The interval of search range may be evaluated as follows. If the photographs are exposed vertically and at the same height, the relation of the x-parallax difference Δp_x and the height difference ΔH between 2 ground points p_1, p_2 is expressed by the well-known formula[14] (see Fig.6):

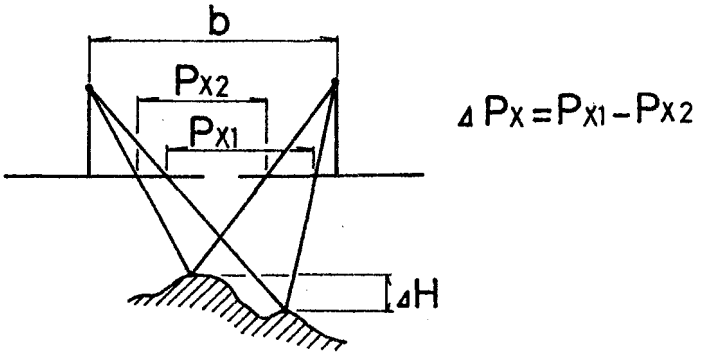

Fig.6 Relation between the x-parallax Difference and the Height Difference

$$\Delta H = \frac{H}{B} \Delta p_x, \tag{5}$$

where $\Delta p_x = p_{x1} - p_{x2}$, p_{x1} and p_{x2} being the x-parallaxes of the photographic points corresponding to p_1 and p_2 respectively. d is the air base measured on the photograph. And H is an exposure height. Let H_m be the maximum height difference which might occur within one patch. Thus follows

$$\Delta p_x \leq \frac{H_m}{H} b. \tag{6}$$

4. Correlation Test and Empirical Improvement

To evaluate the ability of this algorithm, the correlation test was performed on the aerial photographs including mountains, flat lands and valleys. The test area of the photograph is shown in Fig.7, and its data are listed in Table 1. The photograph scale is 1:25,000, which is small enough to allow for unhampered correlation even in the case that there are buildings or trees present.

Table.1 Data about the Photographic Images

Scale	1 : 25,000
Camera	R M K 15/23
Exposure Height	3,800 m
Air Base	87 mm (on the photograph)
Pixel Width	50 μm (1.3 m on the ground)
Output Form	8 bit binary (0-3D)

Fig.7 Photograph of the Plotting Test Area

For digitizing the photographs with high positional accuracy, it is most desirable to use the flat bed mechanical scanner. But by limits of the accomodation of the laboratory, the drum scanner (Joyce Loebl Scangig 3) was used in the test. However, even if the flat bed scanner were available, it might have been of no practical use, since its scanning speed is extremely slow.

A pair of images were digitized with spacing of 50μm ($=d$) and output in 8 bit binary form to MTs. The spacing of 50μm might be rather large considering the photogrammetric reguirement.

The pair of (digital) images are then rectified with the orientation parameters input exogeneously. At the same time the film deformations, which had occured when the films were wound around the drum, were also corrected. In the rectified images the residual y_c-parallaxes of 1 pixel were found in many positions, and 2 pixel were found in a few positions. There y_c-parallaxes are due to incomplete corrections of the film deformations.

In this test, a correlation patch in the first step is a rectangle of about 360 m (in X_G) x 240 m (in Y_G) on the ground including 2 marginal areas. The interval of the search is set at $\pm$ 6 pixel$_i$ for the i-th step. According to E_q.(6), the x_c-parallax of $\pm$ 6 pixel$_1$ corresponds to the height difference on the ground

$$\Delta H \leqq \frac{3{,}800 \text{ m} \times 12 \text{ pixel}_1 \times 0.2 \text{ mm}}{87 \text{ mm}} = 105 \text{ m},$$

since the $pixel_1$ width is 0.2 mm. Therefore, when the correlations begin, the conjugates of nodal points surely can be involved in the respective search range of $\pm$ 6 $pixel_1$, since in this case there exist no height differences of 105 m within one patch.

(1) Basic Correlation Test

Once the precision of the matches of the conjugates remains low in the first step, the precision no longer will be expected to increase in the subsequent steps. Hence the variations of correction amounts of x_c-parallaxes and maximum correlation coefficients were observed while the correlation cycle was repeated in the first step. The result of the test follows;

1) In the flat region, consisting of cultivated land, the x_c-parallaxes converged to the correct values rapidly. In the hilly region, however, dispersions of the x_c-parallaxes were often observed at the corners of the patch as the correlations were iterated a few times. Since each x_c-parallax was estimated independently of those of surrounding nodal points, the positional inversions of the conjugates broke out at many positions. The obtained maximum correlation coefficients in correct matchings were at most 0.5 in the flat land, and 0.4 in the hilly region. However, the correlation coefficients in mismatchings in the hilly region also indicate almost the same values as in the correct matchings. This means the S/N ratios of aerial photographic images is considerably low, especially in featureless hilly regions, and it might be hard to judge if the matching is correct or not only by correlation coefficients.

(2) Parallax Filter

In order to prevent nodal points from having inverted the estimated x_c-parallaxes must be filtered such that the x_c-parallax of the concerned nodal point is replaced by the average of 4 x_c-parallaxes of the neighbours and itself (see Fig.8). At first the filtering had been confined to the points which committed the positional inversion. But the filtering proved to have no negative effects on the correct matching the x_c-parallaxes which converge to a positive value. Thus all the x_c-parallaxes were filtered homogeneously eachtime all the points were correlated once. As a result, no positional inversions occured in any of the steps, and further, the dispersion phenomenon at

the corners of patches disappeared in almost all instances except a few cases in hilly regions.

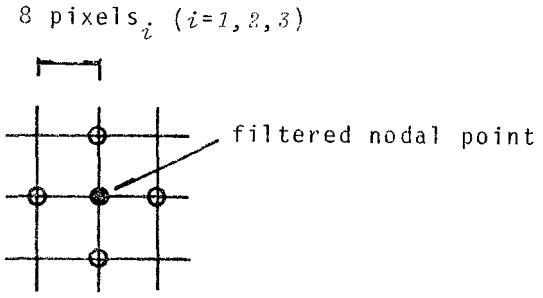

Fig.8 Parallax Filter
The x_c-parallax of a central nodal point is replaced by the average of those of sorrounding 4 points and itself.

(3) Search Range

Up until this time $\pm$ 6 pixels$_i$ (i=1, 2, 3) were used at the search range. But since a correlation sequence consists of only 32 pixels$_i$, estimated positions of correlation peaks apparently lack reliablility. It is widely said that for stable estimation of correlation functions, the sequences should be ten times as long as the required maximum lag. With smaller search range, as a matter of course, the correlation leads to false matchings in many positions. For improving the S/N ratios, two-dimensional windows should be used instead of sequences, in sofar as they do not hurt the sensitivity of pinpointing the minute conjugate positions. How large a window is appropriate, then? Though this is a serious problem, it will not be encompassed in this report as it digresses from the main subject of study.

(4) Wide Area Test

The entire plotting area was devided into 24 patches and then processed. Some empirical tests showed that the iterative correlation process converged by 3 or 4 times for each step. Then for each steps, 5 correlation cycles were iterated. The x_c-parallax file was produced

and from this the contours were plotted in the scale of 1:10,000 as shown in Fig.9. The contour map of the same scale covering the area is shown in Fig.10. Further, a rough size of one correlation patch in the first step is depicted in Fig.9, scaled to the map. The contour lines in both maps closely coincide except in the featureless hilly region.

It took about 67 sec. of cpu time for processing one patch. In the expended time, 26 sec. was taken for transmission of data from the peripheral devices to the memory.

6. Conclusion

This paper describes the algorithm for automatic stereo plotting by iterative image correlation and the empirical test results. The concluding remarks are as follows:

1) The obtained contour plot is very similar to that of the cartographic map except at some places in the featureless hilly region.

2) By filtering the estimated x_c-parallaxes, the positional inversions of conjugates of nodal points and almost all dispersions in correlation, could be avoided. For preventing the dispersion which tends to occur as the correlations go into detail, the correlation structure should be improved. This would require that coarse matching and detail matching could be simultaneously performed in the second and third steps so that the former may control the corrections of x_c-parallaxes to keep the matching from dispersions in the latter.

3) The offered algorithm is not yet satisfactory in that the line matching method with low S/N ratios is extensively used. For obtaining higher S/N ratios in correlation, area matching should be used together with line matching, and for that purpose the more efficient calculation algorithm should be developed.

Acknowledgment

We would like to acknowledge the assistance of Mr. O. Uchida (Asia Aerial Survey Co. Ltd.) who contributed to the troublesome computer programming involved in this work.

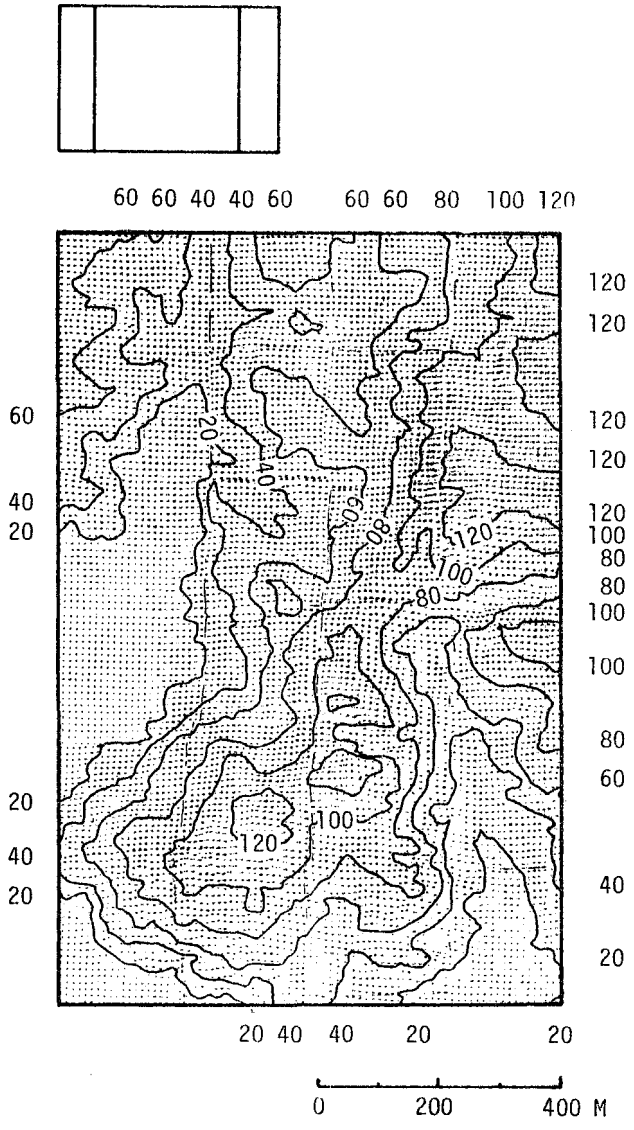

Fig.9 Contour Map Plotted from the x_c-parallax File
A rectangle above the map shows the size
of a correlation patch in the *1*st step.

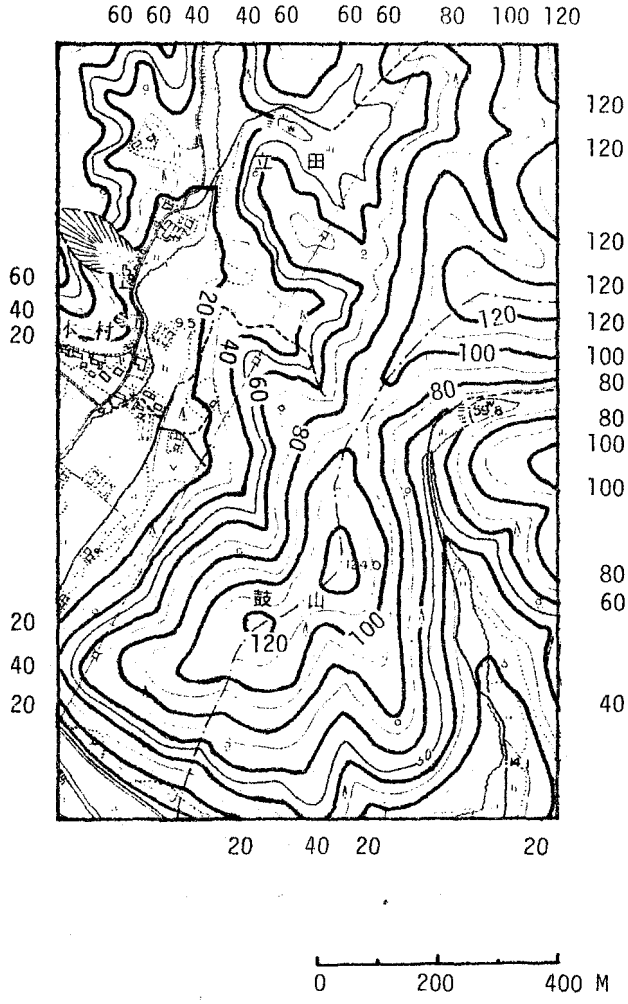

Fig.10 Contour Map of the Test Area

References

1. R. E. Kelly and P. R. H. McConnel, The gestalt photomapping system, *Photogrammetric Engineering & Remote Sensing*, Vol.43, No.11, 1977, pp. 1407-1417.
2. U. V. Helava, US-1 Universal Stereo Plotter, XIII International Congress for Photogrammetry, 1976, Helsinki.
3. H. K. Szangolies, W. Kunze, W. Tiedeken, H. Martin and W. Marckwardt, Topomat, XIII International Congress for Photogrammetry, 1976, Helsinki.
4. G. Konecny and D. pape, Correlation techniques and devices,*Photogrammetric Engineering & Remote Sensing*, Vol.47, No.3, 1981, pp. 323-333.
5. C. Mori, S. Hattori, K. Imai and I. Ogawa, Automatical contour production using image correlation of aerial stereo photographs-Processing and automatic orientation (in Japanese), *Photogrammetric Engineering & Remote Sensing* (Journal of the Japan Society of Photogrammetry), Vol.20, No.4, 1981, pp.4-13.
6. C. Mori, S. Hattori, O. Uchida and H. Tanabe, Automatical contour production using image correlation of aerial stereo photographs— Digital Rectification and height file production (in Japanese), *Photogrammetric Engineering & Remote Sensing* (Journal of the Japan Society of Photogrammetry), Vol.21, No.2, 1982, pp.4-14
7. K.Mori, M. Kidode and H. Asada, An iterative prediction and correction method for automatic stereocomparison, *Computer Graphics and Image Processing*, Vol.2, 1973, pp. 393-401.
8. T. J. Keating, P. R. Wolf and F. L. Scarpace, An improved method of digital image correlation, *Photogrammetic Engineering & Remote Sensing*, 1975, pp. 993-1002.
9. D. J. Panton, A flexible approach to digital stereo mapping,*Photogrammetric Engineering & Remote Sensing*, Vol.44, No.12, 1978, pp. 1499-1512.
10. C. Mori, S. Hattori and H. Tanabe, Rectification of digitized aerial photographic image, *Memoirs of the School of Engineering, Okayama University*, Vol.16, No.1, 1981, pp.47-64.
11. W. Kreiling, Off-line Correlation in General Purpose Computers, Symposium über den Einsatz digitaler Komponenten in der Photogrammetrie, 1978, Hannover.
12. M. J. Hannah, *Computer Matching of Areas in Stereo Images*, Stanford Artificial Intelligence Laboratory Memo AIM-239, Stanford University, 1974.

13. J. W. Cooley, P. A. W. Lewis and P. D. welch, The fast fourier transform and its application to time series analisys, in *Statistical Methods for Digital Computers* (A. Ralston, Ed.), Vol.3, pp. 377-423., Wiley Interscience Pub., New York, 1977.
14. P. R. Wolf, *Elements of Photogrammetry*, pp. 143-175., McGraw-Hill New York, 1974.